Antibiotic production is organized by a division of labour in *Streptomyces*

Zheren Zhang, Frederique de Barsy, Michael Liem, Apostolos Liakopoulos, Young H. Choi, Dennis Claessen*, Daniel E. Rozen*[1]

Institute of Biology, Leiden University, Sylviusweg 72, 2333 BE, Leiden, The Netherlands

- * co-senior authors
- [1] author for correspondence

Abstract

One of the hallmark behaviors of social groups is division of labour, where different group members become specialized to carry out complementary tasks. By dividing labour, cooperative groups of individuals increase their efficiency, thereby raising group fitness even if these specialized behaviors reduce the fitness of individual group members. Here we provide evidence that antibiotic production in colonies of the multicellular bacterium *Streptomyces coelicolor* is coordinated by a division of labour. We show that *S. coelicolor* colonies are genetically heterogenous due to massive amplifications and deletions to the chromosome. Cells with gross chromosomal changes produce an increased diversity of secondary metabolites and secrete significantly more antibiotics; however, these changes come at the cost of dramatically reduced individual fitness, providing direct evidence for a trade-off between secondary metabolite production and fitness. Finally, we show that colonies containing mixtures of mutant strains and their parents produce significantly more antibiotics, while colony-wide spore production remains unchanged. Our work demonstrates that by generating mutants that are specialized to hyper-produce antibiotics, streptomycetes reduce the colony-wide fitness costs of secreted secondary metabolites while maximizing the yield and diversity of these products.

Introduction

Social insects provide some of the most compelling examples of divisions of labour, with extremes in morphological differentiation associated with highly specialized functions and reproductive sterility in all colony members except the queen [1]. However, conditions that select for division of labour are not limited to animals and it has become increasingly clear that microbes offer unique opportunities to identify and study the mechanistic underpinnings of divisions of labour [2–7]. First, microbes are typically clonal, which helps ensure that a division of labour is favoured by kin selection [3]. Second, microbial populations are highly social, often cooperating to carry out coordinated behaviors like migration or biofilm formation that require the secretion of metabolically expensive public goods that can be shared among clonemates [8,9]. If these conditions are met, and investment in public good secretion trades-off with fitness, divisions of labour are predicted to evolve [3,10].

Here we describe the cause and evolutionary benefits of a unique division of labour that has evolved in colonies of the filamentous actinomycete *Streptomyces coelicolor*. After germinating from uni-chromosomal spores, these bacteria establish multicellular networks of vegetative hyphae, reminiscent of fungal colonies [11,12]. Vegetative hyphae secrete a broad variety of public goods, such as chitinases and cellulases that are used to acquire resources, as well as a chemically diverse suite of antibiotics that are used to kill or inhibit competing organisms [13–15]. Streptomycetes are prolific producers of antibiotics, and are responsible for producing more than 50% of our clinically relevant antibiotics [11]. Although the terminal differentiation of *Streptomyces* colonies into vegetative hyphae (soma) and viable spores (germ) is well understood [16], no other divisions of labour in these multicellular bacteria are known. However, opportunities for phenotypic differentiation are possible, because even though colonies begin clonally, they can become genetically heterogeneous because of unexplained high-frequency rearrangements and deletions in their large, ~9 Mb linear chromosome [17–21]. The work we describe shows that these two topics are intertwined. Briefly, we find that genomic instability causes irreversible genetic differentiation within a subpopulation of growing cells. This in turn gives rise to a division of labour that increases the productivity and diversity of secreted antibiotics and increases colony-wide fitness.

Results

Genome instability and phenotypic heterogeneity are coupled

Genome instability and phenotypic heterogeneity have been observed in several *Streptomyces* species [18,22], but there are no explanations for the evolution or functional consequences of this extreme mutability. To begin addressing this question, we quantified the phenotypic heterogeneity arising within 81 random single colonies of *S. coelicolor* M145 by harvesting the spores of each of these colonies and then replating the collected spores onto a new agar surface. Although most progeny are morphologically homogeneous and similar to the wild-type, strikingly aberrant colonies (Figure 1a) arise at high frequencies (0.79 +/- 0.06%, mean +/- SEM, ranging from 0% to 2.15%) (Figure 1a). To determine the heritability of these aberrant phenotypes, we restreaked 15 random colonies from different plates onto a new agar plate which revealed a remarkably variability in colony morphology (Figure 1b). Rather than reverting to the wild-type (WT) morphology, as would be anticipated if the initial heterogeneity were due to phenotypic plasticity or another form of bistability, the colonies derived from mutant colonies are themselves hypervariable, giving rise to up to nine diverse

81 phenotypes from any single colony. Thus, in the course of two cycles of colony outgrowth, an array of
82 colony types emerged that differ in size, shape and colour (Figure 1b). Because our ability to discern
83 colony heterogeneity is limited to only a few visually-distinct phenotypic characters, we assume that
84 these estimates of diversity are lower than their true level of occurrence.

85 Using whole-genome sequencing of 8 random mutants we confirmed that these isolates contained
86 profound chromosomal changes. As shown in Figure 2a, large genome deletions were observed at the
87 chromosome ends in all 8 strains. In 3 cases we found an ~297 kb amplification on the left
88 chromosomal arm flanked by the Insertion Sequence IS1649, encoced by SCO0091 and SCO0368.
89 Average sequence coverage of the amplified region suggests it contains between 2 and 15 copies of
90 this amplification (Figure 2a and S1). Sequencing results were expanded using pulsed-field gel
91 electrophoresis (PFGE) analysis of 30 additional mutant isolates (Figure 2b and S2). Consistent with our
92 sequencing results, this analysis revealed that mutants contained variably sized deletions of either up
93 to ~ 240 kb or ~ 872 kb on the left chromosome arm, while deletions to the right chromosome arm
94 extended to up to 1.6 Mb, deleting more than 1,000 genes. Additionally, 8/30 strains contained the
95 same large amplification between copies of IS1649 as noted above. Interestingly, these strains are
96 conspicuously yellow, which might be caused by the overproduction of carotenoids due to the
97 amplification of the *crt* gene cluster (SCO0185-0191;[11,23,24]). In addition to this and other phenotypic
98 effects associated with these changes that are discussed below, deletions to the right chromosome
99 arm cause the loss of two loci, *argG* (SCO7036) and *cmlR1*(SCO7526)*/cmlR2*(SCO7662), that result in
100 two easily scorable phenotypes: arginine auxotrophy and chloramphenicol susceptibility, respectively.
101 Scoring these phenotypes allows rapid determination of the minimal size of the deletion on the right
102 chromosome arm in the absence of molecular characterization. Chloramphenicol susceptibility
103 indicates a deletion of at least 322 kb, while the addition of arginine auxotrophy indicates a deletion
104 of at least 843 kb (Figure 2b).

105 ***Mutants increase the production and diversity of antibiotics***

106 Mutant strains are conspicuously pigmented when compared to their parental wild-type strains (Figure
107 1). Because many secondary metabolites, including antibiotics, produced by *S. coelicolor* are
108 pigmented, e.g. actinorhodin and prodigines which are blue and red, respectively, we tested if mutant
109 strains had altered secondary metabolite profiles. Secreted metabolites from mutant and WT strains
110 grown on agar surfaces were analyzed using ^{1}H NMR profiling [25]. Principal component analysis (PCA)
111 (Figure 3a) supports the partition of strains into three well-separated groups: wild-type and wild-type-
112 like strains, and then two clusters of mutant isolates. In each case, groupings correspond to the size of
113 genomic lesions mentioned above. More specifically, strains grouping in the wild-type and wild-type-
114 like cluster are chloramphenicol resistant (Cam^{R}) and arginine prototrophic (Arg^{+}), while those
115 clustering within the blue ellipse are chloramphenicol susceptible (Cam^{S}) and protrophic for arginine
116 (Arg^{+}), and those in the red-ellipsed cluster are susceptible to chloramphenicol (Cam^{S}) and auxotrophic
117 for arginine (Arg^{-}).

118 We next asked if these different metabolic profiles translated to differences in biological activity,
119 specifically the production of antibiotics that inhibit the growth of other bacteria. Thirty mutant strains
120 were grown on agar plates and then covered with a soft-agar overlay containing *B. subtilis*. Inhibition
121 was visualized as an absence of growth surrounding the mutant colony, and the extent of inhibition
122 was determined from the size of the inhibition zone. As shown in Figure 3b, all but three WT-like

mutant strains produced significantly larger zones of inhibition than the WT strain (One-tailed t-tests, all $p < 0.05$). In addition, we observed significant heterogeneity among mutant strains in halo size (One-Way ANOVA, $F_{29,90} = 5.45$, $p < 0.001$).

These results indicate that mutant strains produce more antibiotic than their wild-type parent when assayed against a single bacterial target. However, they do not distinguish if strains can be further partitioned on the basis of which other species they inhibit. Score plots of princiapl component analysis based on ^{1}H NMR signals reveal clear separation between mutant clones within and between clusters (Figure 3a), suggesting that their killing spectra may vary. To test this, we chose 4 representative mutant clones, one from each of the different PCA groupings, and then measured their ability to inhibit 48 recently isolated *Streptomyces* strains [26]. *Streptomyces* targets were chosen because these are likely to represent important competitors for other streptomycetes in soil environments. Against 40 out of 48 targets, at least one of the four mutant strains produced a significantly larger halo than the wild-type strain, indicating increased antibiotic production (Figure 3c). More interestingly, for these 40 targets, we observed significant differences between the mutant strains themselves. We found differences in the size of the zone of inhibition on different target species (Two-Way ANOVA, $F_{39,117} = 21.79$, $p < 0.001$) as well as a significant interaction between mutant strain and the target species (Two-Way ANOVA, $F_{117,320} = 5.75$, $p < 0.001$), indicating that the inhibitory profiles of each mutant strain is distinct from the others. Together these results reveal that mutants arising within colonies are not only better killers, but that they are also diversified in who they can kill because their killing spectra do not overlap. They also suggest that the beneficiary of diversified antibiotic secretion is the parent strain, because competing bacteria are unlikely to be resistant to this broadened combination of secreted antimicrobials.

To test if the increased inhibition we observed against *B. subtilis* was correlated with the ^{1}H NMR profiles we obtained, we used a partial least squares (PLS) regression (Figure 3d) [25,27], which showed that the separation into different groups significantly correlates with halo size ($Q^2 = 0.879$) which was further validated by both permutation-tests and ANOVA of cross-validated residuals (CV-ANOVA, $F_{8,116} = 104.443$, $p < 0.001$). To identify possible compounds that are overproduced in mutants compared to WT, we identified several ^{1}H NMR signals that vary across strains and strongly correlated with the size of the zone of inhibition against *B. subtilis* (Table S1); notable among these are several aromatic signals which might correspond to the blue-pigmented antibiotic, e.g. actinorhodin, which have activity against some Gram-positive bacteria [28,29].

Antibiotic production is coordinated by a division of labour

Having shown that *Streptomyces* colonies differentiate into distinct subpopulations that vary in their antibiotic production, we next asked how this differentiation affects colony fitness. To answer this, we measured the fitness of each mutant strain by quantifying the number of spores they produce when grown in isolation. As shown in Figure 4a, mutants produce significantly fewer spores than the wild-type strain (all $p < 0.001$) and, in extreme cases, as much as 10,000-fold less, with significant heterogeneity among strains (One-Way ANOVA: $F_{29,59} = 132.57$, $p < 0.001$). Importantly, the reduction in spore production is significantly negatively correlated with antibiotic production ($F_{1,29} = 26.51$, $r^2 = 0.478$, $p < 0.001$) (Figure S3). This provides evidence that antibiotic production is metabolically costly to *S. coelicolor* and that there is a direct trade-off between antibiotic production and reproductive capacity. In addition, we observed a significant negative correlation between the size of the genome

deletion and CFU ($F_{1,7} = 12.32$, $r^2 = 0.638$, $p = 0.0099$) and a positive correlation between deletion size and bioactivity against *B. subtilis* ($F_{1,7} = 37.97$, $r^2 = 0.844$, $p < 0.001$), suggesting that these phenotypes scale with the magnitude of genomic changes (Figure 4b).

To examine the effects of mutant strains on the colony as a whole, we mixed mutant strains with their parent at increasing frequencies and quantified colony-wide spore production and the ability of these mixtures to kill *B. subtilis*. Results of these experiments, shown in Figure 4c, support two important conclusions: 1) increasing fractions of mutants lead to increased antibiotic production; and 2) even though mutant strains have individually reduced fitness (Figure S3), their presence within colonies has no effect on colony-wide spore production, until the mutant frequency exceeds > 50% of the total. We carried out the same assay with 3 additional mutant clones, but at fewer frequencies to estimate spore production, and observed concordant results (Figure S4): up to a frequency of ~ 50%, mutant strains have no effect on colony-wide spore production, while each incremental increase in the frequency of these strains enhances colony-wide antibiotic output. These results indicate that the benefits of producing cells with chromosomal lesions are evident across a broad range of frequencies, but that even with extremely high mutation rates the costs to colony-wide fitness are minimal or entirely absent.

Discussion

Streptomycetes are prolific producers of antibiotics, with genomes typically containing more than 20 secondary metabolite gene clusters that comprise more than 5% of their entire genome [11,30]. They invest heavily in these products and their biosynthesis and secretion is costly. Our results suggest that by limiting antibiotic production to a fraction of the colony through division of labour, *S. coelicolor* can eliminate the overall costs of biosynthesis while maximizing both the magnitude and diversity of their secreted antibiotics. Although this comes at a large individual cost, it increases group fitness by improving the ability for *S. coelicolor* to kill or inhibit their competitors. Moreover, our results reveal that the range of conditions that select for a division of labour are quite broad, because colony-wide fitness is unaffected, even if mutant strains are as frequent as ~ 50%.

Division of labour is predicted to be favoured in this system for several reasons. First, *Streptomyces* colonies emerge from a single spore and are clonal [16]. This, together with their filamentous mode-of-growth, ensures that costly individual traits can be maintained due to their indirect fitness benefits [3,4,31]. And because resistance to the diversified antibiotic profile of mutant strains is unlikely to be present in competing strains, only the parent strain stands to benefit from their sacrifice. Second, the costs of antibiotic production via large and dedicated multi-step biosynthetic pathways, e.g. non-ribosomal peptide or polyketide synthases, are likely to be highest at the initiation of antibiotic production but diminish thereafter, meaning that producing cells become more efficient at making antibiotics through time [10]; furthermore, we show that antibiotic production trades-off with reproduction. Finally, many antibiotics are secreted, so the entire colony, but not susceptible competitors, can benefit from the protection they provide [15].

Even if conditions predispose to a division of labour, there must still be a process that generates phenotypic heterogeneity. Our results show that in *Streptomyces*, this is caused by genomic instability that creates a subpopulation of cells within colonies that contain large deletions or amplifications at the termini [18,20,21]. Importantly, these mutations are severe and irreversible. Because strains, or

206 portions of colonies, containing these deletions have significantly reduced fitness, they effectively
207 behave like a sterile caste that provide direct benefits to the rest of the colony and receive little in
208 return [1]. Indeed, even when the initial frequency of mutants in mixed colonies approaches 80%, their
209 final frequency declines to less than 1% after one cycle of colony growth (Figure S5). This suggests that
210 the division labour in *S. coelicolor* is re-established independently and differently in each colony, a
211 mechanism that may help to maximize the diversity of secreted antibiotics.

212 It remains unclear if there are mechanisms regulating the size and frequency of chromosomal deletions
213 and amplifications. One possibility is that these events are induced by external environmental
214 conditions and that their rate is context dependent. Instability can be elevated by exposure to certain
215 toxicants, e.g. mitomycin C or nitrous acid [32], although no explicit stress was added in the experiments
216 we report. It may also be increased during competition with other strains, a process that is known to
217 alter the secretion of secondary metabolites [14,33]. Another possibility is that deletions, and the benefits
218 they bring for antibiotic production, are a fortuitous byproduct of the programmed cell death that
219 accompanies development [16]. By this argument, chromosome degradation would be regulated, but
220 wouldn't always be lethal. Although we have not confirmed this experimentally, it is likely that
221 conserved amplifications result from the flanking copies of IS1649, which can facilitate intragenomic
222 rearrangements [34]. In either case, the expectation is that increased antibiotic production results from
223 the deregulation of biosynthetic clusters following the deletion of 100s of genes, many known to
224 coordinate antibiotic biosynthesis [11]. And because deletions are stochastic, especially following the
225 removal of protective telomeres at the ends of linear chromosomes, this would also cause antibiotic
226 production to vary in different sections of the colony.

227 Our preliminary surveys have found similar levels of genomic instability in streptomycetes strains we
228 have freshly isolated from soil, suggesting that the division of labour we describe here is general. We
229 are limited, however, in our ability to detect polymorphisms; color changes are conspicuous and are
230 invariably associated with changes to pigmented secondary metabolites, but other secreted public
231 goods may also become modified in these multicellular bacteria. Understanding which, if any other,
232 public goods vary in the ways shown here is crucial because it will help to identify conditions that lead
233 to a genetically encoded division of labour as compared to other forms of regulation that allow
234 complex multicellular microbial systems to coordinate their behaviors and maximize their fitness.

235 Acknowledgements

236 We acknowledged the helpful comments of Christian Kost, Shraddha Shitut, and Sanne Westhoff on
237 an earlier version of this manuscript and assistance with bioinformatics and NMR analysis from Chao
238 Du and Lina Bayona. We also thank Gilles van Wezel for access to wild Streptomyces isolates.
239 Funding was provided by the China Scholarship Council (CSC) to Z.Z., by the JPI-AMR to A.L and D.E.R.
240 and by NWO to D.C.

241 Author contributions

242 Z.Z., D.C. and D.R. conceptualized and planned the study. Z.Z. and F.d.B.collected data. All authors
243 analyzed and interpreted the results. Z.Z., D.C. and D.R. drafted the manuscript with input from the
244 other authors. All authors approved the final submitted version of this paper.

245

Competing interests

The authors declare there are no competing interests.

Materials and Methods

Bacterial strains and growth conditions

Streptomyces coelicolor was cultivated at 30 °C on Soy Flour Mannitol Media agar plates (SFM) for strain isolation and to quantify CFU [35]. SFM contains, per liter: 20 g mannitol, 20 g agar and 20 g soya flour. To examine antibiotic production and to extract secondary metabolites, we used minimal media (MM) supplied with 0.5% mannitol and 740 µg ml^{-1} casamino acids. MM contains, per liter, 0.5 g L-asparagine, 0.5 g K_2HPO_4, 0.2 g $MgSO_4.7H_2O$, 0.01 g $FeSO_4.7H_20$ and 10 g agar. For DNA extraction, strains were grown in liquid flasks shaken at 200 rpm at 30 °C in TSBS:YEME (1:1 v:v) supplemented with 0.5% glycine and 5mM $MgCl_2$. TSBS contains 30 g tryptic soya broth powder and 100 g sucrose/liter. And YEME contains 3 g yeast extract, 5 g peptone, 3 g malt extract, 10 g glucose and 340 g sucrose. *E. coli* and *B. subtilis* were cultivated at 37 °C in LB media with constant shaking or on LB-agar plates.

All strains were derived from a single isolate of *S. coelicolor* A3(2) M145 (designed as WT). Briefly, samples from a frozen spore stock were streaked onto SFM agar to obtain single colonies. After 5-days of growth, 81 single colonies with WT morphology were restreaked onto another SFM plate. From each plate single colonies with conspicuously mutant phenotypes were picked into sterile water and plated at appropriate dilutions onto SFM agar (n = 3/colony), from which we estimated the frequency of different mutant phenotype classes. Each derived type was plated to confluence on SFM agar, and after 7 days of growth, spores were harvested to generate spore stocks which were stored at -80 °C in 20% glycerol.

Phenotypic scoring

Two phenotypes that are related to the loss of loci in the right arm were scored (n = 3 /strain). The arginine auxotrophs were identified by replicating 10^3 CFU of each strain on MM supplied with 0.5% Mannitol with and without 37 µg ml^{-1} arginine[32]. After 5 days of growth, auxotrophs were identified as those strains that only grow on the media supplied with arginine. Chloramphenicol resistance was estimated by using the disk diffusion method. In detail, $2x10^5$ spores were spread onto MM supplemented with 740 µg ml^{-1} casamino acids [32] in 12 mm square petri dishes, followed by placing a paper disk containing 25 µg chloramphenicol on it. After 4 days, the radius of the inhibition zone around the disk was measured using ImageJ [36]. Inhibition zones that were smaller than 5 mm were scored as resistant while those that are larger than 5 mm were scored as susceptible.

Antibiotic production

Spores of each strain were diluted to 10^5 CFU ml^{-1} in MiliQ water and 1 µl was spotted onto MM + casamino acids agar plates (n = 4/strain). After growth for 5 days at 30 °C, plates were covered with 15 ml of LB soft agar (0.7%) containing 300 µl of a freshly grown indicator strain (OD_{600} 0.4-0.6). After overnight incubation at 30 °C, zones of inhibition around producing colonies were measured using ImageJ.

285 The bioactivity against *Streptomyces* isolates was tested for four strains, 2H1A, 8H1B, 9H1B and 9H1A.
286 Three ml of SFM agar was poured onto each well of a 5x5 grid plate (Griener), after which we spotted
287 1 µl of each test strain containing ~10^6 total spores in the corner of each well. After 5-day growth, 500
288 µl of MM supplemented with 0.5% mannitol and 740 µg ml^{-1} casamino acids containing ~10^5 spores of
289 the target strain was overlaid on top. Zones of inhibition were measured 2 days later using ImageJ.
290
291 ***^{1}H NMR profiling and data analysis***

292 2x10^5 spores were spread onto MM + casamino acids in 12 mm square petri dishes (n=3/strain). After
293 5-days of incubation at 30 °C, agar was chopped into small pieces using a sterile metal spatula and
294 secreted compounds were extracted in 50 ml ethyl acetate for 72h at room temperature. Next, the
295 supernatant was poured off and evaporated at 37 °C using a rotating evaporator. Pellets were obtained
296 by drying at room temperature to remove extra solvents and then freeze-dried to remove remaining
297 water. After adding 500 µl methanol-d_4 to the dried pellets, the mixtures were vortexed for 30 seconds
298 followed by a 10-minute centrifugation at 16000 rpm. The supernatants were then loaded into a 3
299 mm- NMR tube and analyzed using 600 MHz ^{1}H NMR (Bruker, Karlsruhe, Germany)[25].

300 Data bucketing of NMR profiles was performed using AMIX software (version 3.9.12, Bruker Biospin
301 GmbH) set to include the region from δ 10.02 to 0.2 with a bin of 0.04 ppm scaled to total intensity,
302 while the signal regions of residual H_2O in methanol (δ 4.9 – 4.7) and methanol (δ 3.34 – 3.28) were
303 excluded. Multivariate data analysis was performed with the SIMCA software (version 15, Umetrics,
304 Sweden).

305 ***CFU production***

306 To quantify CFU, 10^4 spores of each strain were spread onto SFM agar (n = 3/strain, except n = 2 for
307 9H1B) and left to grow for 7 days to confluence. After 7 days, spores were harvested by first adding 10
308 ml MilliQ water onto the plate and then using a cotton swab to remove spores and mycelial fragments
309 from the plate surface. Next, the water suspension was filtered through an 18 gauge syringe plugged
310 with cotton wool to remove mycelial fragments. After centrifuging the filtered suspension at 4000 rpm
311 for 10 min, the supernatant was poured off and the spore pellet was dissolved in a total volume of 1ml
312 20% glycerol. CFU per plate was determined via serial dilution onto SFM agar.

313 ***DNA extraction and sequencing***

314 Nine strains, including one wild-type and eight mutants, were selected for sequencing with the Sequel
315 system from Pacific Bioscience (PacBio, USA). Roughly 10^8 spores were inoculated in 25 ml TSBS:YEME
316 (1:1 v:v) supplemented with 0.5% glycine and 5 mM $MgCl_2$ and cultivated at 30°C with 200 rpm shaking
317 speed overnight. The pellet was then collected after centrifugation and washed twice with 10.3%
318 sucrose. Samples were then resuspended in DNA/RNA shield (Zymo Research, USA) with 10x volume
319 at room temperature and sent to be commercially sequenced at Baseclear (Leiden, The Netherlands).

320 Subreads of the sequenced results shorter than 50 bp were filtered and stored in BAM format. The
321 reference alignments were performed against *Streptomyces coelicolor* A3(2) genome (NC_003888.3)
322 using BLASR (v5.3.2) [37]. Resulting BAM files were then sorted and indexed using SAMtools (v1.9) [38] .
323 For the calculation of genome rearrangements, the depths were called and exported through the
324 depth function in SAMtools. The edges of genome were identified by manually checking the break
325 point where the coverage drops to zero. The size of the amplified region was defined by the

326 dramatically higher coverage compared to the adjacent sequences. All results were further confirmed
327 by visualizing them in IGV (v2.4.15) [39].

328 ***Pulsed-field gel electrophoresis (PFGE)***

329 Approximately 10^8 spores were inoculated into 25 ml TSBS:YEME (1:1 v:v) supplemented with 0.5%
330 glycine and 5 mM $MgCl_2$ and cultivated overnight at 30 °C at 200 rpm. After centrifuging the culture
331 at 4000 rpm for 10 min, the pellet was resuspended in 400 µl cell suspension buffer containing 100
332 mM Tris: 100mM EDTA at pH 8.0 and 1 mg ml^{-1} lysozyme and mixed with the same volume of 1%
333 SeaKem Gold Agarose (Lonza, USA) in TE buffer containing 10 mM Tris: 1 mM EDTA at pH 8.0 with 1%
334 SDS. This mixture was immediately loaded into the PFGE plug mold (Bio-rad, USA). Next, plugs were
335 lysed in 5 ml cell lysis buffer containing 50 mM Tris: 50 mM EDTA at pH 8.0, 1% N-Lauroylsarcosine,
336 sodium salt and 4 mg ml^{-1} lysozyme incubated for 4 hours at 37 °C with gentle agitation. This was then
337 followed by a 5-hour incubation in 5 ml cell lysis buffer containing 0.1 mg ml^{-1} proteinase K at 56 °C
338 and 50 rpm. Finally, the plug was washed twice in pre-heated milliQ water and 4 times in pre-heated
339 TE buffer and incubated at 56 °C for at least 15 min with gentle mixing. Plugs were sliced into 2 mm
340 width pieces and pre-soaked in 200 µl 1x NEB 3.1 buffer for at least 30min. After replacing the buffer
341 with 200 µl 1x NEB 3.1 buffer, 2 µl of the rare-cutter AseI (New England Biolabs, UK) was added and
342 incubated at 30 °C overnight. 1% agarose was used for running fragments in 0.5x freshly prepared TBE.
343 0.225-2.2 Mb *S. cerevisiae* chromosomal DNA (Bio-rad, USA) and wild-type *S. coelicolor* DNA were used
344 as size markers for estimate fragment sizes. Two electrophoresis conditions were applied to separate
345 and visualize the smaller (<1016 kb) and larger fragments (>1016 kb): (Switch time: 2.2-75 s; Voltage:
346 200 V; Running time: 19 h) and (Switch time: 60-125 s; Voltage: 200 V; Running time: 20 h), respectively.

347 PFGE results were compared to the AseI restriction maps of the wild-type strain which contains 17
348 fragments ranging from 26bp to 1601 kb (Figure S2). Two fragments, 240 kb and 632 kb, can be easily
349 resolved if they are deleted from the left arm while one large 1601 kb fragment can be affected when
350 deletions occur in right arm.

351 ***Fitness assay***

352 The relative fitness of four fully sequenced mutant isolates, 2H1A, 8H1B, 9H1B and 9H1A, was
353 estimated during pairwise competition with the wild-type parent. To distinguish strains, we first
354 transformed mutant and wild-type strains with the integrating plasmids PIJ82 and pSET152 which
355 confer hygromycin B and apramycin resistance, respectively. Potential fitness effects of the markers
356 were determined by generating two WT variants that were transformed with either single marker. No
357 effects were observed in these control experiments (One sample t-test, $t = 2.029$, $df = 7$, $p = 0.082$).
358 Fitness assays were initiated by normalizing each strain to a density of 10^6 spores/ml and then mixing
359 at different starting ratios of Mutant:WT. 100 µl of this mixture, containing 10^5 spores, was plated as
360 a lawn onto SFM agar and incubated at 30 °C for 5 days, while another fraction of the sample was
361 plated after serial dilution onto SFM containing either 50 µg ml^{-1} apramycin or 50 µg ml^{-1} hygromycin
362 B to precisely quantify the densities of each strain. After 5 days of growth, bacteria were harvested as
363 above and plated by serial dilution onto SFM containing either 50 µg ml^{-1} apramycin or 50 µg ml^{-1}
364 hygromycin B. Fitness was quantified, following Lenski et al [40], by calculating the ratio of the Malthusian
365 parameters of both strains. Values below 1 indicate that mutant strains have lower fitness than the
366 WT strain. More detailed assays were carried out with strain 9H1A, where we simultaneously
367 estimated the fitness of this strain at a broader range of frequencies from 10-99% and determined

368 how the frequency of the mutant strain influenced antibiotic production, as measured by the size of
369 the zone of inhibition against a *B. subtilis* indicator in a soft agar overlay.

370 References

371 1. Robinson, G. E. Regulation of Division of Labor in Insect Societies. *Annu. Rev. Entomol.* **37**,
372 637–665 (1992).

373 2. Gestel, J. V. a N., Vlamakis, H. & Kolter, R. Division of Labor in Biofilms : the Ecology of Cell
374 Differentiation. *Microbiol. Spectr.* **3**, 1–24 (2015).

375 3. West, S. A. & Cooper, G. A. Division of labour in microorganisms: an evolutionary perspective.
376 *Nat. Rev. Microbiol.* (2016). doi:10.1038/nrmicro.2016.111

377 4. Zhang, Z., Claessen, D. & Rozen, D. E. Understanding microbial divisions of labor. *Front.*
378 *Microbiol.* **7**, 1–8 (2016).

379 5. Kim, W., Levy, S. B. & Foster, K. R. Rapid radiation in bacteria leads to a division of labour. *Nat.*
380 *Commun.* **7**, 10508 (2016).

381 6. Dragoš, A. *et al.* Division of Labor during Biofilm Matrix Production. *Curr. Biol.* **28**, 1903–
382 1913.e5 (2018).

383 7. Dragoš, A. *et al.* Collapse of genetic division of labour and evolution of autonomy in pellicle
384 biofilms. *Nat. Microbiol.* **3**, 1451–1460 (2018).

385 8. West, S. A., Diggle, S. P., Buckling, A., Gardner, A. & Griffin, A. S. The Social Lives of Microbes.
386 *Annu. Rev. Ecol. Evol. Syst.* **38**, 53–77 (2007).

387 9. Tarnita, C. E. The ecology and evolution of social behavior in microbes. *J. Exp. Biol.* **220**, 18–24
388 (2017).

389 10. Schiessl, K. *et al.* Individual- versus group-optimality in the production of secreted bacterial
390 compounds. *bioRxiv* 094086 (2016). doi:10.1101/094086

391 11. Bentley, S. D. *et al.* Complete genome sequence of the model actinomycete *Streptomyces*
392 *coelicolor* A3(2). *Nature* **417**, 141–7 (2002).

393 12. Zacchetti, B., Wösten, H. A. B. & Claessen, D. Multiscale heterogeneity in filamentous
394 microbes. *Biotechnol. Adv.* **36**, 2138–2149 (2018).

395 13. Chater, K. F., Biró, S., Lee, K. J., Palmer, T. & Schrempf, H. The complex extracellular biology of
396 *Streptomyces*. *FEMS Microbiol. Rev.* **34**, 171–198 (2010).

397 14. Abrudan, M. I. *et al.* Socially mediated induction and suppression of antibiosis during bacterial
398 coexistence. *Proc. Natl. Acad. Sci. U. S. A.* **112**, 11054–9 (2015).

399 15. van der Meij, A., Worsley, S. F., Hutchings, M. I. & van Wezel, G. P. Chemical ecology of
400 antibiotic production by actinomycetes. *FEMS Microbiol. Rev.* **41**, 392–416 (2017).

401 16. McCormick, J. R. & Flärdh, K. Signals and regulators that govern *Streptomyces* development.
402 *FEMS Microbiol. Rev.* **36**, 206–231 (2012).

403 17. Altenbuchner, J. & Cullum, J. DNA amplification and an unstable arginine gene in
404 *Streptomyces lividans* 66. *Mol. Gen. Genet.* **195**, 134–138 (1984).

405 18. Leblond, P. *et al.* Hypervariability, a new phenomenon of genetic instability, related to DNA
406 amplification in *Streptomyces ambofaciens*. **171**, 419–423 (1989).

407 19. Betzler, M., Dyson, P. & Schrempf, H. Relationship of an Unstable argG Gene to a 5 . 7-
408 Kilobase Amplifiable DNA Sequence in *Streptomyces lividans* 66. 4804–4810 (1987).

409 20. Volff, J. N. & Altenbuchner, J. Genetic instability of the *Streptomyces* chromosome. *Mol.*
410 *Microbiol.* **27**, 239–46 (1998).

411 21. Birch, A., Häusler, A. & Hütter, R. Genome rearrangement and genetic instability in
412 *Streptomyces* spp. *J. Bacteriol.* **172**, 4138–42 (1990).

413 22. Gravius, B., Bezmalinović, T., Hranueli, D. & Cullum, J. Genetic instability and strain
414 degeneration in *Streptomyces rimosus*. *Appl. Environ. Microbiol.* **59**, 2220–8 (1993).

415 23. Krügel, H., Krubasik, P., Weber, K., Saluz, H. P. & Sandmann, G. Functional analysis of genes
416 from *Streptomyces griseus* involved in the synthesis of isorenieratene, a carotenoid with
417 aromatic end groups, revealed a novel type of carotenoid desaturase. *Biochim. Biophys. Acta -*
418 *Mol. Cell Biol. Lipids* **1439**, 57–64 (1999).

419 24. Takano, Hideaki; Obitsu, Saemi; Beppu, Teruhiko; Ueda, K. Light-Induced Carotenogenesis in
420 *Streptomyces coelicolor* A3(2): Identification of an Extracytoplasmic Function Sigma Factor
421 That Directs Photodependent Transcription of the Carotenoid Biosynthesis Gene Cluster. *J.*
422 *Bacteriol.* **187**, 1825–1832 (2005).

423 25. Wu, C., Du, C., Gubbens, J., Choi, Y. H. & van Wezel, G. P. Metabolomics-Driven Discovery of a
424 Prenylated Isatin Antibiotic Produced by *Streptomyces* Species MBT28. *J. Nat. Prod.* **78**, 2355–
425 2363 (2015).

426 26. Zhu, H. *et al.* Eliciting antibiotics active against the ESKAPE pathogens in a collection of
427 actinomycetes isolated from mountain soils. *Microbiol. (United Kingdom)* **160**, 1714–1726
428 (2014).

429 27. Wu, C., Zhu, H., van Wezel, G. P. & Choi, Y. H. Metabolomics-guided analysis of isocoumarin
430 production by *Streptomyces* species MBT76 and biotransformation of flavonoids and
431 phenylpropanoids. *Metabolomics* **12**, 90 (2016).

432 28. Wu, C. *et al.* Expanding the chemical space for natural products by *Aspergillus-Streptomyces*
433 co-cultivation and biotransformation. *Sci. Rep.* **5**, 1–10 (2015).

434 29. Mak, S. & Nodwell, J. R. Actinorhodin is a redox-active antibiotic with a complex mode of
435 action against Gram-positive cells. *Mol. Microbiol.* **106**, 597–613 (2017).

436 30. Challis, G. L. & Hopwood, D. A. Synergy and contingency as driving forces for the evolution of
437 multiple secondary metabolite production by *Streptomyces* species. *Proc. Natl. Acad. Sci. U. S.*
438 *A.* **100 Suppl 2**, 14555–61 (2003).

439 31. Claessen, D., Rozen, D. E., Kuipers, O. P., Søgaard-Andersen, L. & van Wezel, G. P. Bacterial
440 solutions to multicellularity: a tale of biofilms, filaments and fruiting bodies. *Nat. Rev.*
441 *Microbiol.* **12**, 115–124 (2014).

442 32. Volff, J. N., Vandewiele, D., Simonet, J. M. & Decaris, B. Ultraviolet light, mitomycin C and
443 nitrous acid induce genetic instability in *Streptomyces ambofaciens* ATCC23877. *Mutat. Res. -*
444 *Fundam. Mol. Mech. Mutagen.* **287**, 141–156 (1993).

445 33. Traxler, M. F., Watrous, J. D., Alexandrov, T., Dorrestein, P. C. & Kolter, R. Interspecies
446 Interactions Stimulate Diversification of the *Streptomyces coelicolor* Secreted Metabolome.
447 *MBio* **4**, (2013).

448 34. Widenbrant, E. M. & Kao, C. M. Introduction of the foreign transposon Tn4560 in
449 *Streptomyces coelicolor* leads to genetic instability near the native insertion sequence IS1649.
450 *J. Bacteriol.* **189**, 9108–9116 (2007).

451 35. Kieser, T. *et al. Practical Streptomyces genetics*. (John Innes Foundation).

452 36. Rueden, C. T. *et al.* ImageJ2: ImageJ for the next generation of scientific image data. *BMC*
453 *Bioinformatics* **18**, 529 (2017).

454 37. Chaisson, M. J. & Tesler, G. Mapping single molecule sequencing reads using basic local
455 alignment with successive refinement (BLASR): application and theory. *BMC Bioinformatics*
456 **13**, 238 (2012).

457 38. Li, H. *et al.* The Sequence Alignment/Map format and SAMtools. *Bioinformatics* **25**, 2078–
458 2079 (2009).

459 39. Thorvaldsdóttir, H., Robinson, J. T. & Mesirov, J. P. Integrative Genomics Viewer (IGV): high-
460 performance genomics data visualization and exploration. *Brief. Bioinform.* **14**, 178–92 (2013).

461 40. Lenski, R., Rose, M., Simpson, S. & Tadler, S. Long-term experimental evolution in *Escherichia*
462 *coli*. I. Adaptation and divergence during 2,000 generations. *Am. Nat.* (1991).

463

464

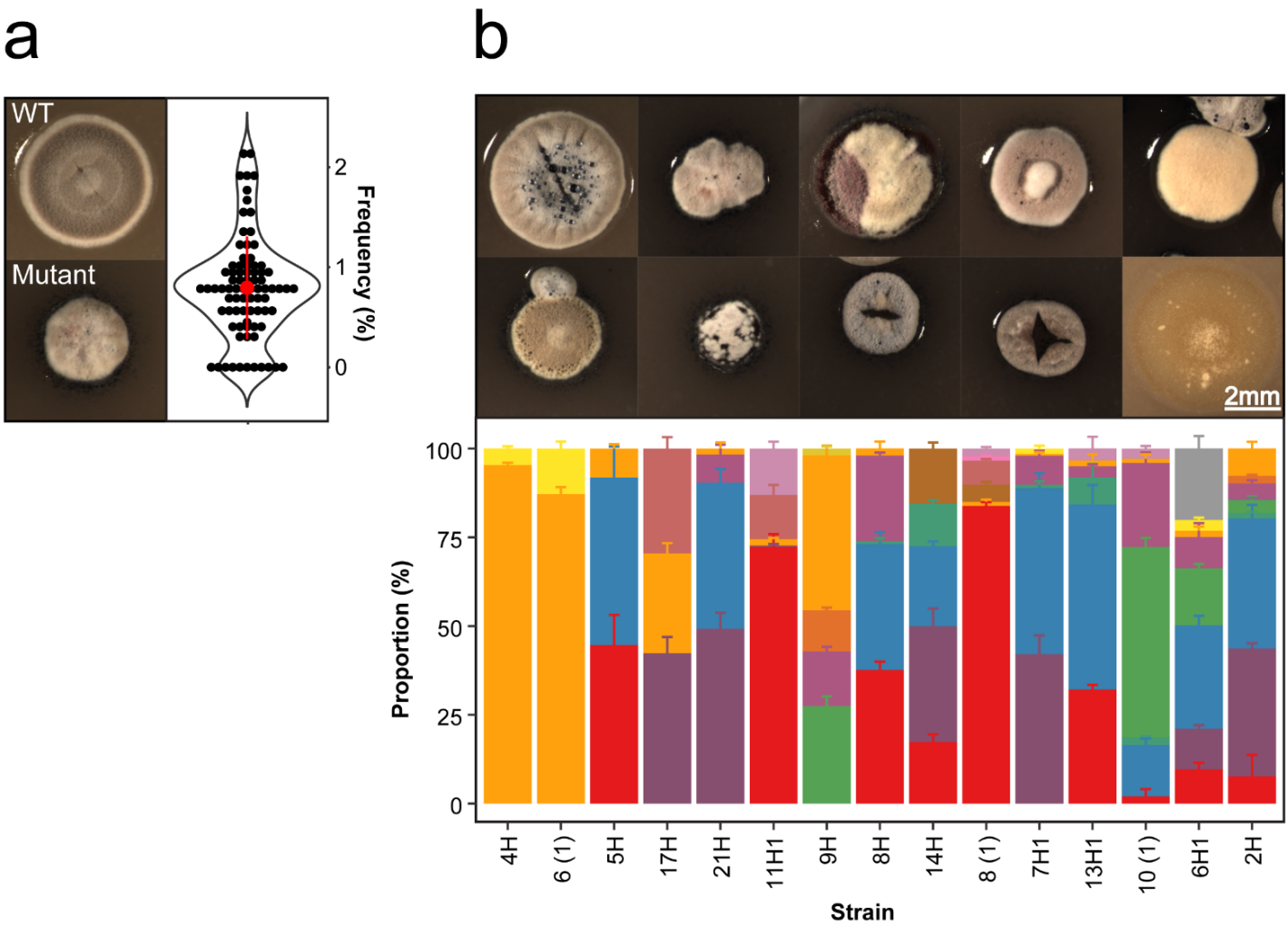

Figure 1: The emergence of phenotypic heterogeneity in colonies of *Streptomyces coelicolor*. (a) Wild-type (top) and mutant (bottom) colonies, and the frequency that mutants emerge from WT colonies (right). (B) Phenotypically diverse progeny (top) emerge after re-streaking mutant colonies that vary in size, shape and pigmentation. Representative colonies are shown. The bottom graph depicts the range of distinct morphologies that emerge after re-streaking 15 random colonies. Each color represents a distinct colony phenotype.

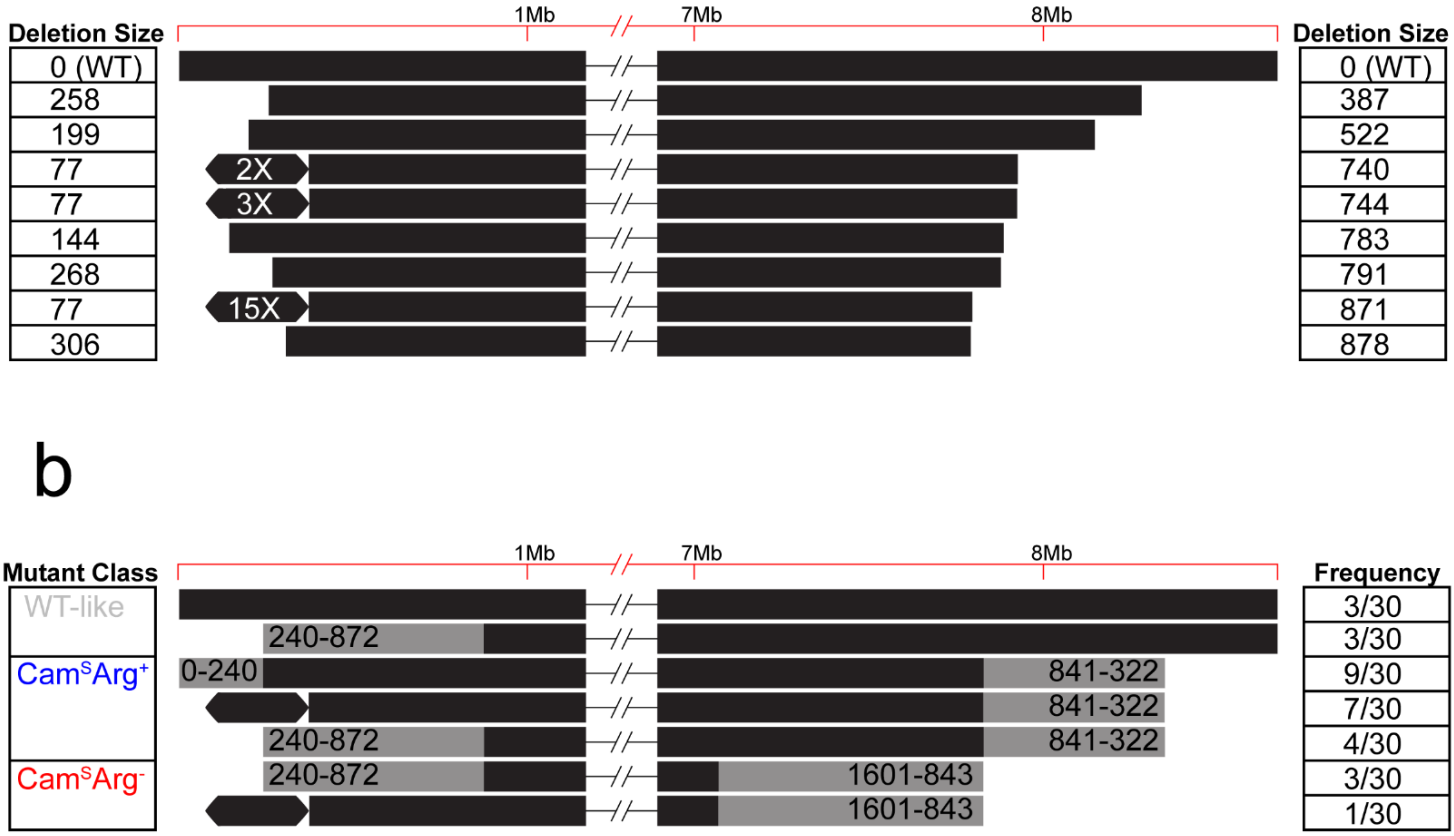

Figure 2: Genome diversity of mutant colonies determined from (a) whole-genome sequencing and (b) Pulsed-field gel electrophoresis (PFGE). Values in (a) correspond to the size (in kb) of genome deletions while the hexagons represent an ~297 kb genome amplification. Each line in (b) depicts the range of deletion sizes (grey) in each mutant class, together with their respective frequencies from 30 sampled mutant strains.

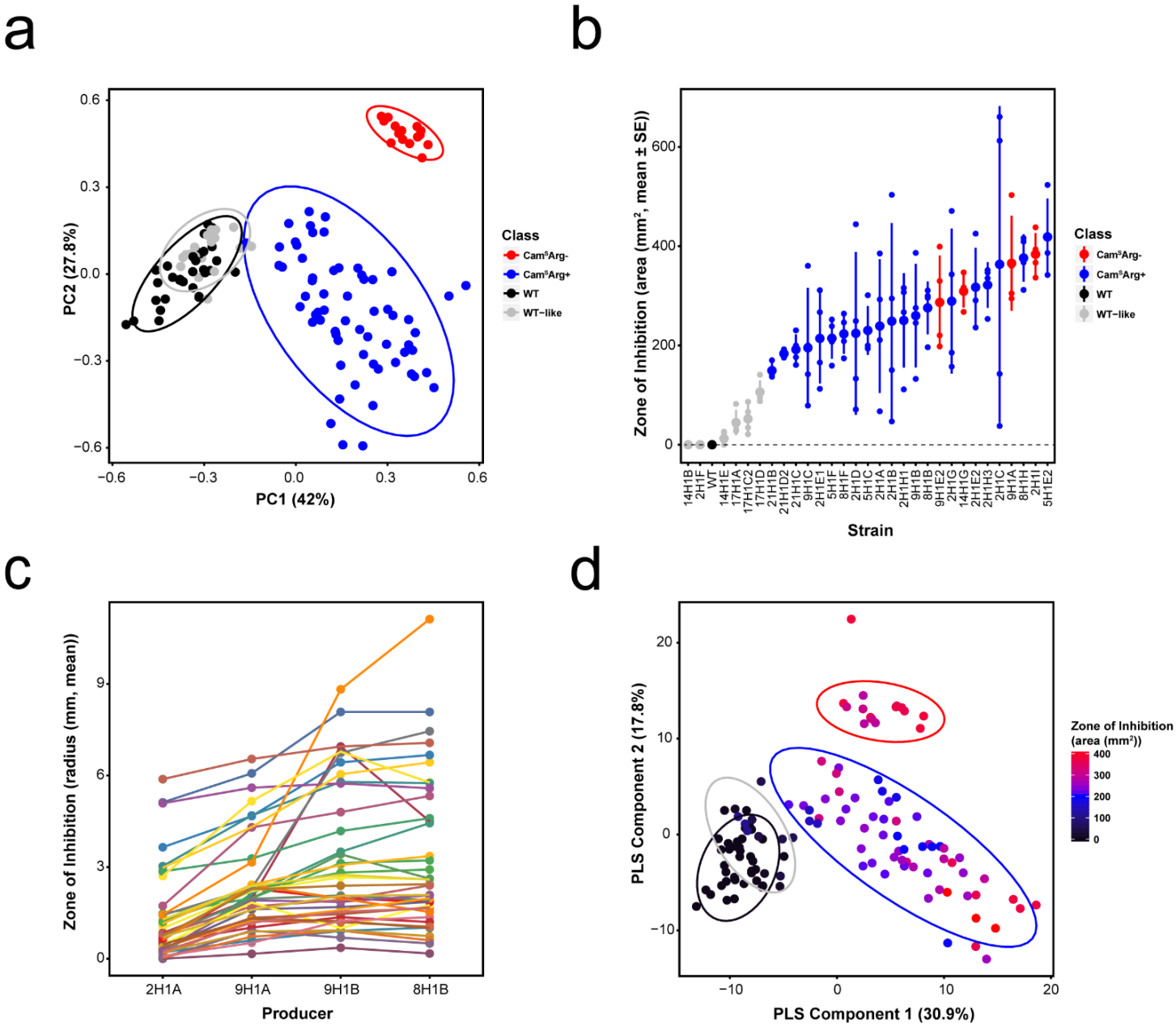

Figure 3: Secondary metabolite production in mutant strains determined by ^{1}H NMR (a and d) or based on either zones of inhibition on *B. subtilis* (b) or 40 different natural streptomycete isolates (c). (a) PCA plot of ^{1}H NMR data. Each cluster enclosed in a colored ellipse (with 95% CI) corresponds to a mutant class with a different phenotype and degree of genomic instability: WT-like strains (in grey), Cam^{S}Arg$^+$ strains (in blue) and Cam^{S}Arg$^-$ strains (in red). (b) Zones of inhibition of each strain when grown with a *B. subtilis* soft-agar overlay. Colors represent the same mutant classes as in (a). The large dot represents the mean of four replicates while the error bar represent the standard error of mean. (c) Zones of inhibition of 4 representative mutant strains with an overlay of 40 different natural streptomycetes, each represented by a different line. (d) PLS plot of ^{1}H NMR data partitioned by the same clusters as in (a). The heat map indicates the size of the zone of inhibition on *B. subtilis.* Statistics are given in the main text.

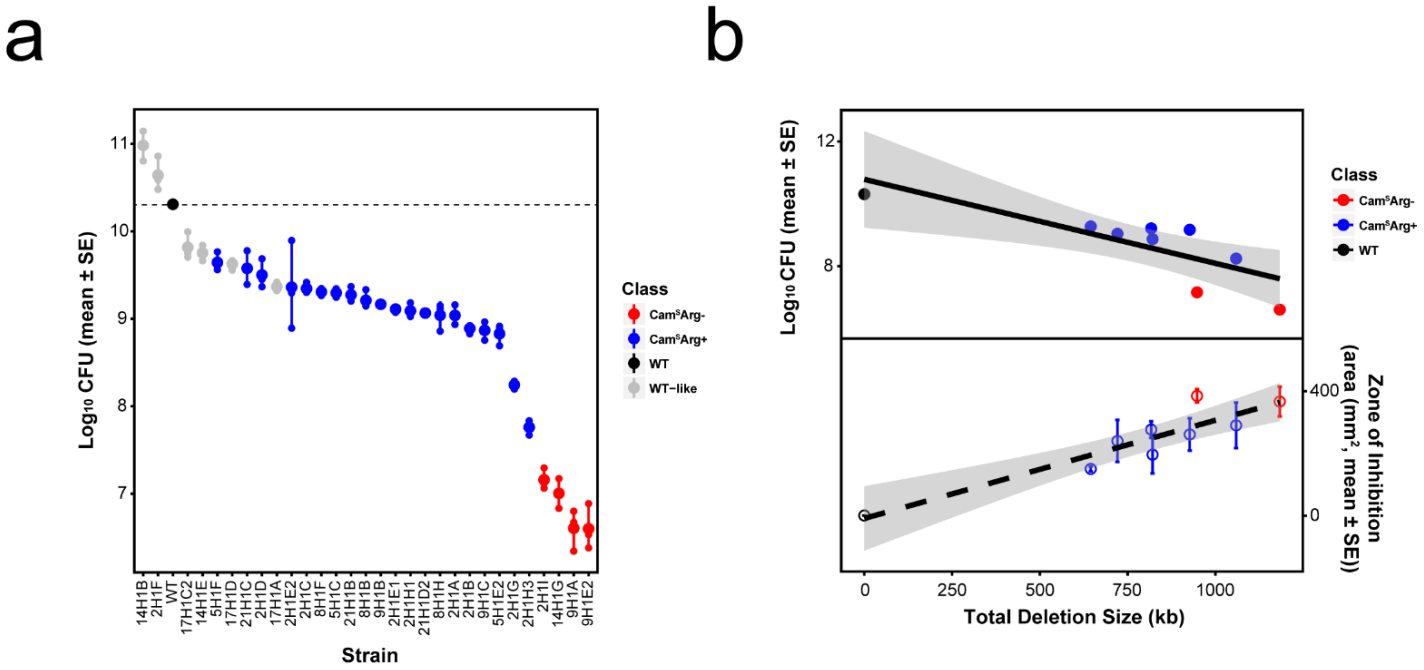

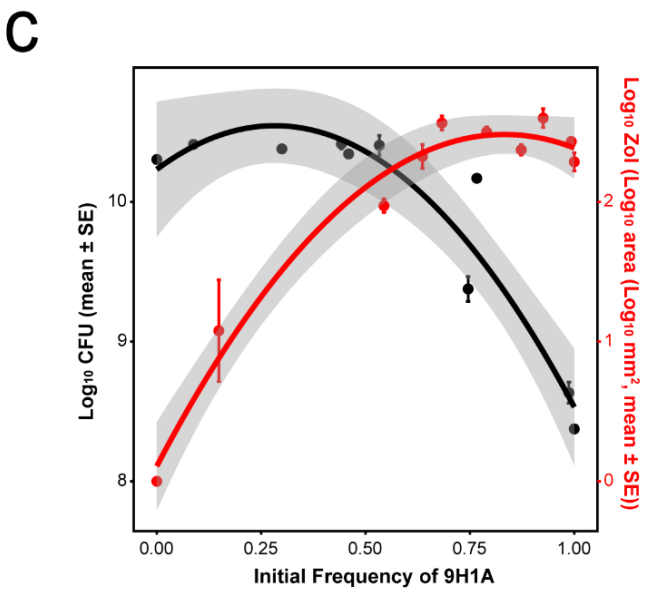

Figure 4: (a) Fitness (CFU) of mutant strains**.** (b) Decreases in genome size negatively correlate with fitness (top panel) and positively correlate with antibiotic production (lower panel). (c) Division of labour during co-culture of the WT and strain 9H1A at different starting frequencies. Increasing frequencies of 9H1A cause increased antibiotic production ($F_{2,7}$ = 37.95, r^2 = 0.916, $p < 0.001$) (red), but only negatively impact colony fitness at frequencies > ~ 50% ($F_{2,13}$ = 131.7, r^2 = 0.953, $p < 0.001$) (black). Quadratic regression lines include the 95% CI.

Supplemental figures:

Antibiotic production is organized by a division of labour in *Streptomyces*

Zheren Zhang, Frederique de Barsy, Michael Liem, Apostolos Liakopoulos, Young H. Choi, Dennis Claessen*, Daniel E. Rozen*[1]

Institute of Biology, Leiden University, Sylviusweg 72, 2333 BE, Leiden, The Netherlands

- * co-senior authors
- [1] author for correspondence

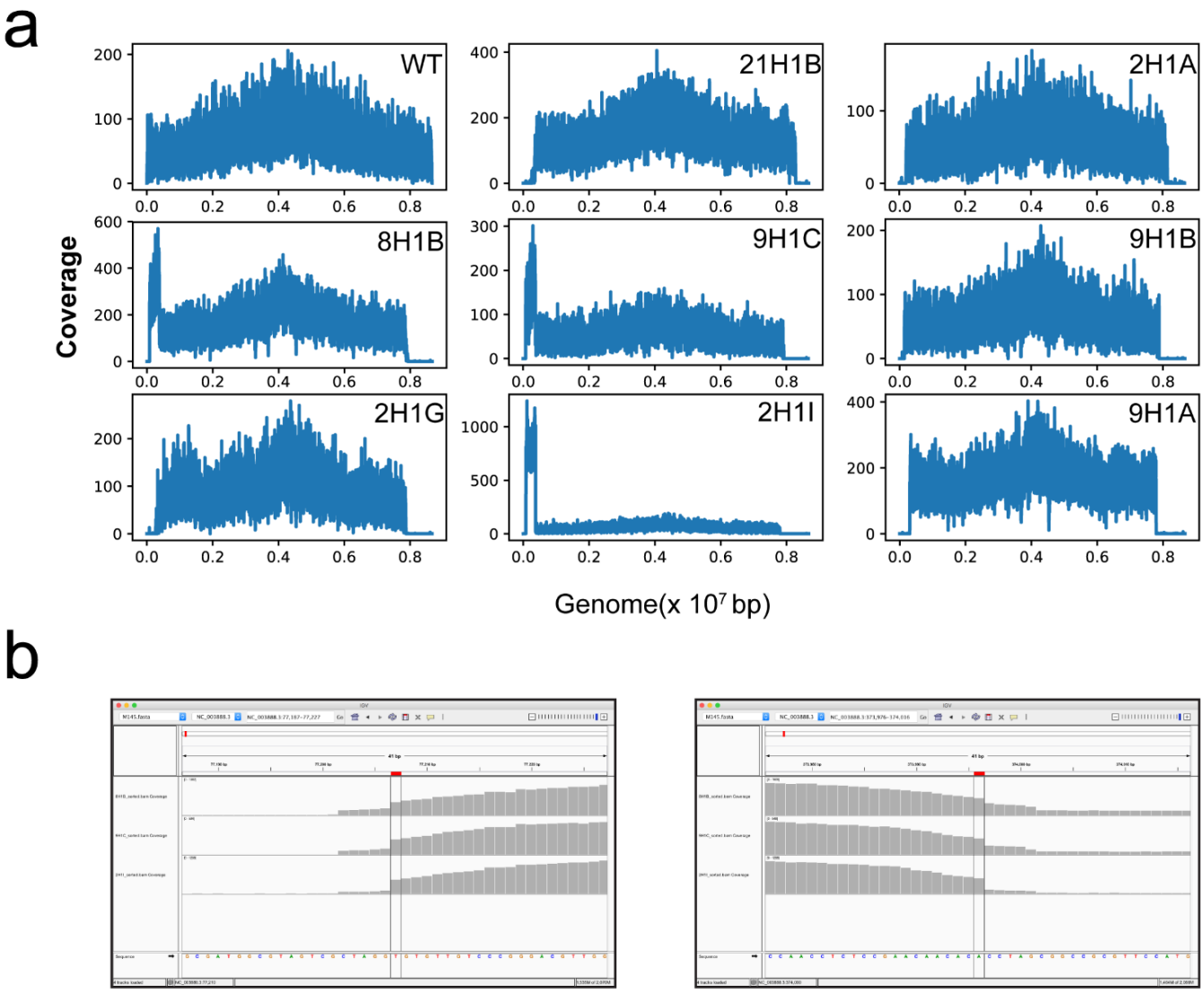

Figure S1:
(a) PacBio reads mapped to the *S. coelicolor* M145 reference genome indicating coverage and highlighting breakpoints for genome deletions, where coverage declines to 0, as well as the size of the conserved amplified regions on the left chromosomal arms of strains 8H1B, 9H1C and 2H1I. (b) IGV snapshots of the left and right borders of amplified regions of strains 8H1B, 9H1C and 2H1I.

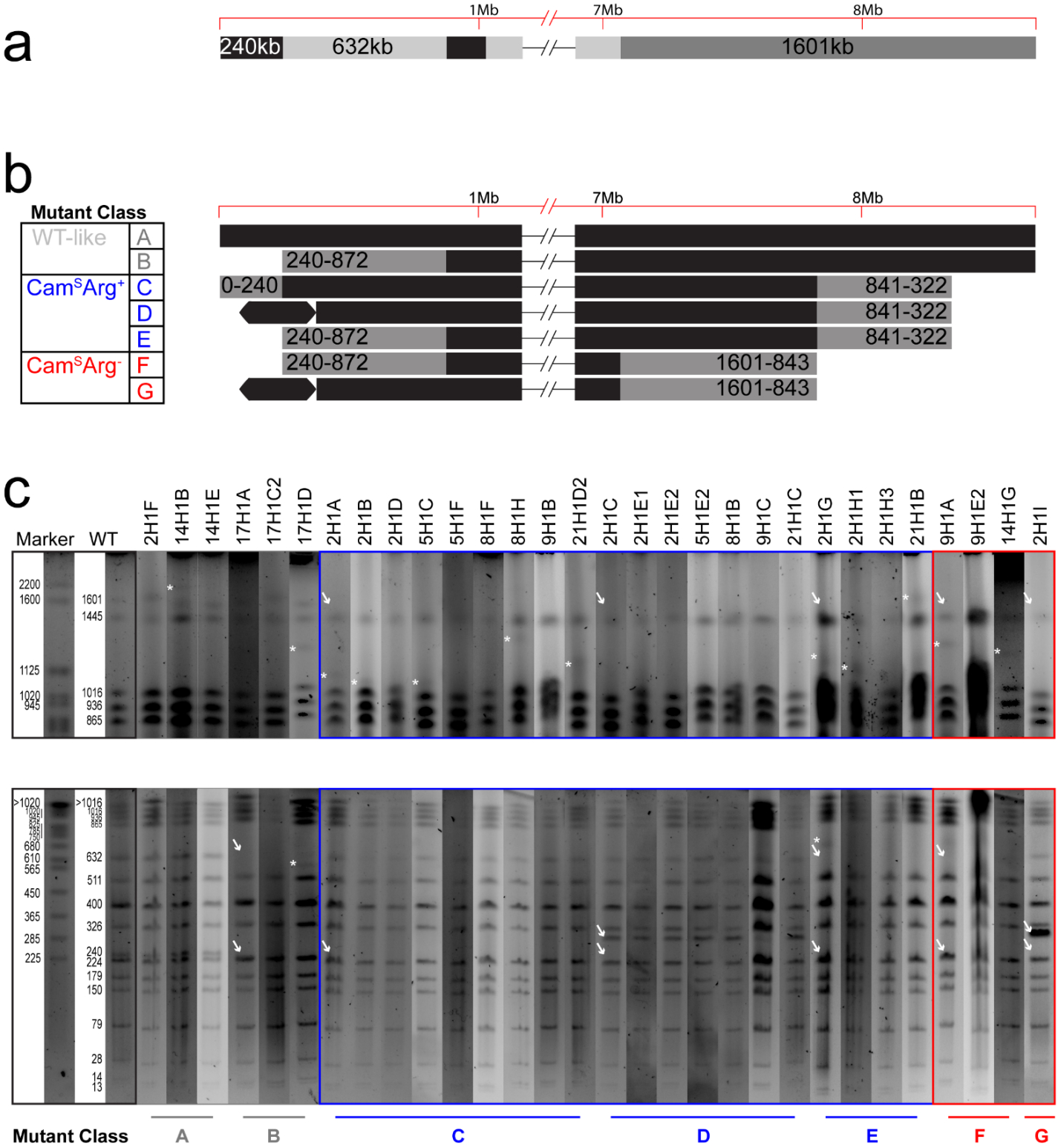

Figure S2: Pulse field gel electrophoresis (PFGE) results of all sampled strains. (a) The schematic of changes to *S. coelicolor* fragments in mutant isolates after AseI digestion. Two bands (240 kb and 632 kb) and one 1601 kb band can be affected on the left and right arms, respectively. (b) Schematic adjusted from Figure 2b with more detailed mutant classes, designated A-G. (c) PFGE results of 30 sampled strains. Two running conditions are used to visualize larger (top panel) or smaller (bottom panel) fragments. (Detailed running conditions are given in the Materials and Methods). White arrows indicate missing or newly appearing of the bands for different mutant class. Asterisks indicate the new bands that were used to evaluate precise genome length.

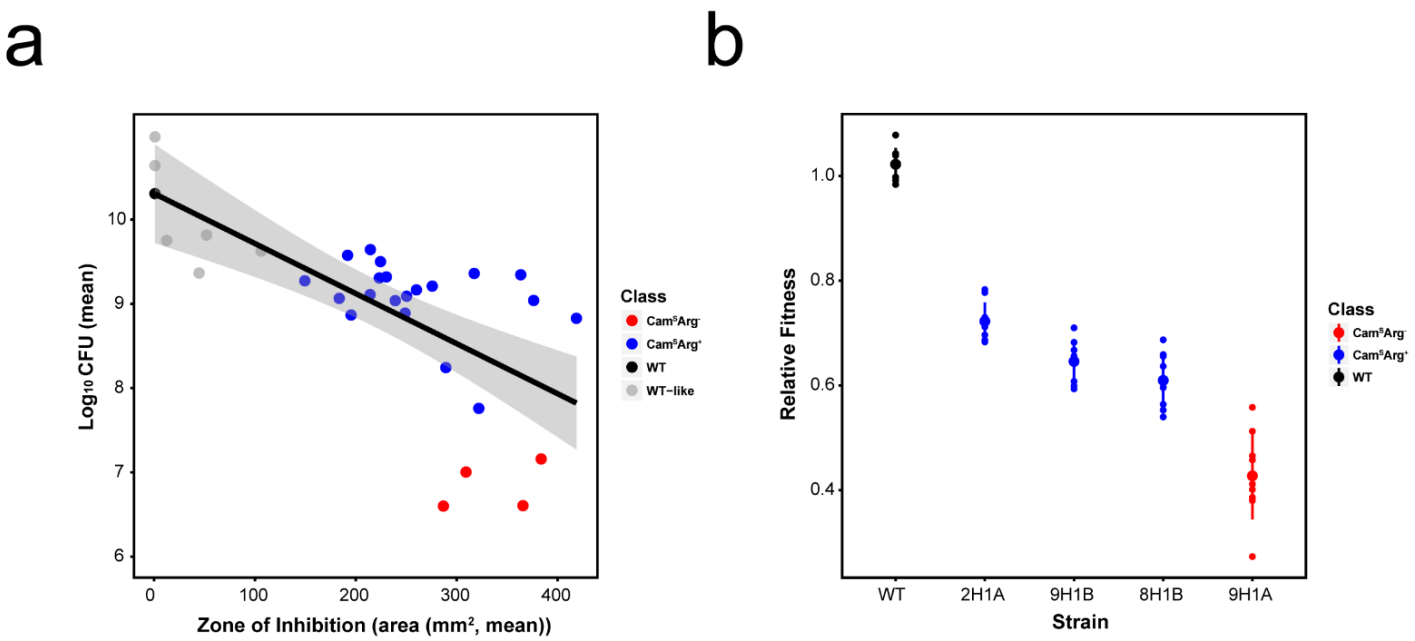

Figure S3: (a) The trade-off between antibiotic production and reproductive capacity, partitioned by different mutant classes. (b) Relative fitness of four selected strains. Detailed methods are given in the Methods and Materials.

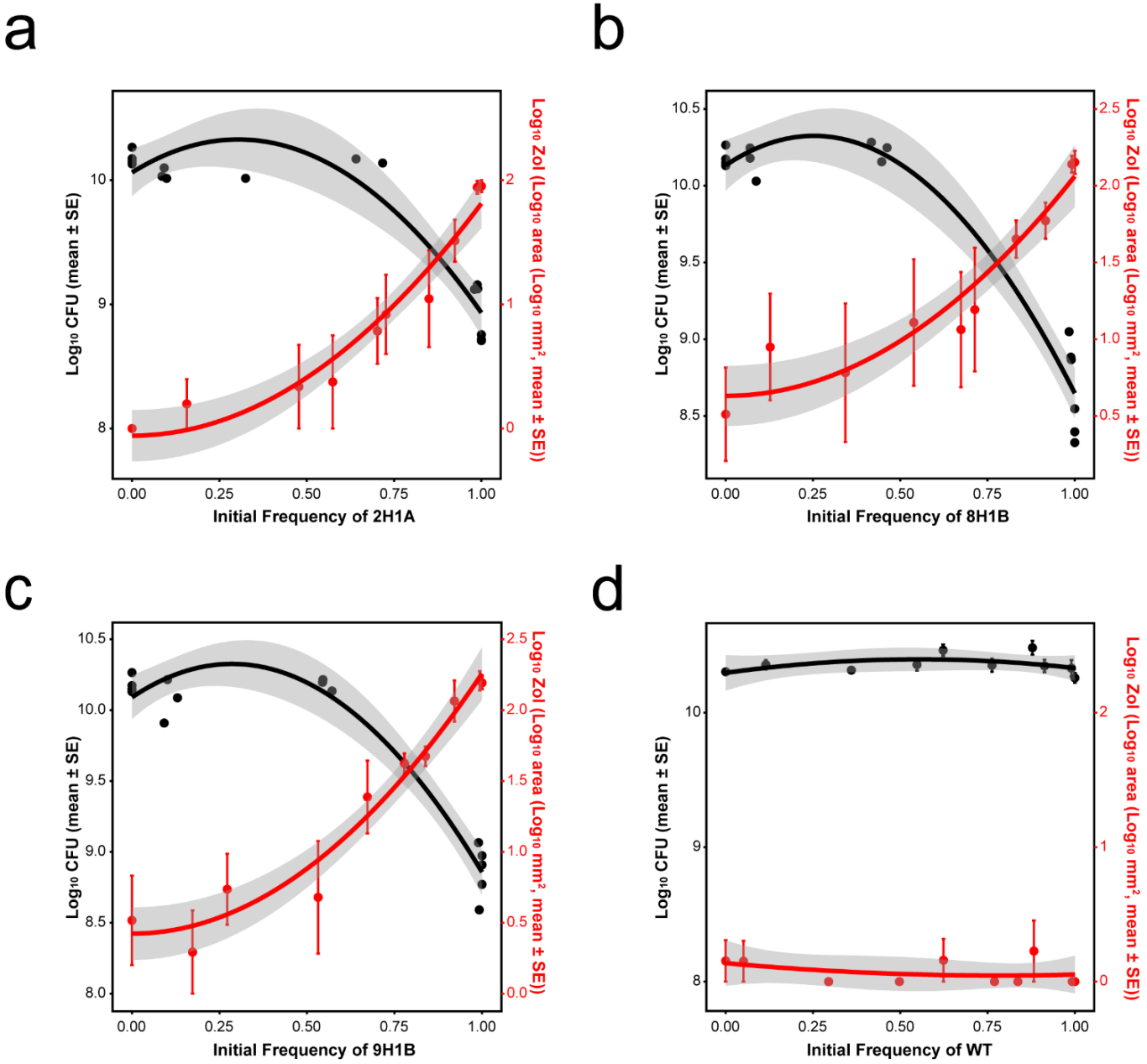

Figure S4. Extended evidence for division of labour during co-culture of the WT and three mutant strains at different starting frequencies. Increasing frequencies of mutants cause increased antibiotic production (red) for (a) 2H1A ($F_{1,8}$ = 170.3, r^2 = 0.955, $p < 0.001$), (b) 8H1B ($F_{1,8}$ = 105.3, r^2 = 0.929, $p < 0.001$) and (c) 9H1B ($F_{1,8}$ = 201.1, r^2 = 0.962, $p < 0.001$) but not (d) WT ($F_{2,7}$ = 0.576, r^2 = 0.141, p = 0.587). Increasing frequencies of mutants only negatively impact colony fitness at frequencies > ~ 50% (black) for (a) 2H1A ($F_{2,13}$ = 59.44, r^2 = 0.901, $p < 0.001$), (b) 8H1B ($F_{2,13}$ = 131.7, r^2 = 0.953, $p < 0.001$) and (c) 9H1B ($F_{2,12}$ = 201.1, r^2 = 0.944, $p < 0.001$) but not (d) WT ($F_{2,7}$ = 1.076, r^2 = 0.235, p = 0.391). Quadratic regression lines include the 95% CI.

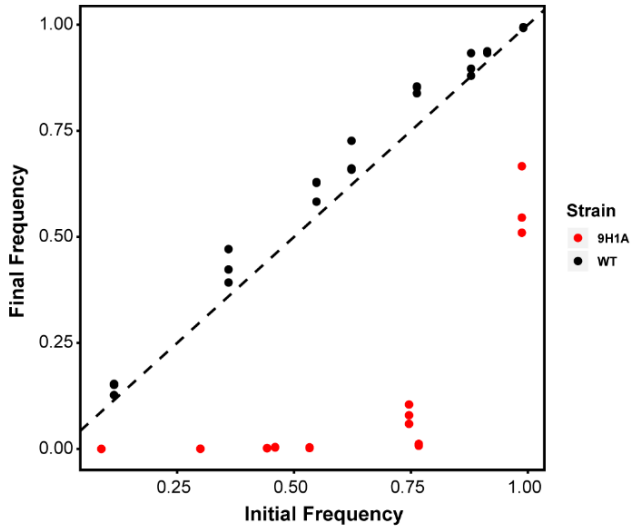

Figure S5: Initial and final frequencies of strains during pairwise competition assays between 9H1A (red) and the wild-type or between two differentially marked wild-type strains (black). The dashed line indicates that initial and final frequencies are equal, while values below the line indicate that the competing strain has declined during the competition assay. While the differentially marked wild-type strains have equal fitness, the mutant strain has dramatically reduced fitness at every starting frequency.

Signal	w*c [1]	SE
2.56	0.123	0.022
2.80	0.115	0.031
1.56	0.110	0.021
7.20	0.109	0.019
7.40	0.106	0.009
2.84	0.105	0.013
Zone of Inhibition	0.105	0.031
7.28	0.105	0.015
7.12	0.103	0.010
7.24	0.103	0.019
8.00	0.101	0.017

Table S1: The ten signals with highest X and Y weights (w* and c) for PLS component 1. The association with the zone of inhibition on *B. subtilis* suggests their contribution to increased killing.